Journal of the European Ceramic Society **18** (1998) 95–104

PII: S0955-2219(97)00089-7
0955-2219/98/$19.00 + 0.00

Monitoring of the Corrosion of YSZ by Impedance Spectroscopy

C. M. S. Rodrigues,[a] J. A. Labrincha[b] and F. M. B. Marques[b]*

[a] Polythecnic Institute of Viana do Castelo, ESTG4900, Viana do Castelo, Portugal
[b] Ceramics and Glass Engineering Dept., University of Aveiro, 3810 Aveiro, Portugal

(Received 6 January 1997; accepted 27 February 1997)

Abstract

Mixtures of yttria-stabilized zirconia (YSZ) with a soda-lime glass and different types of alumina were co-fired at high temperature (1500°C) before characterization by impedance spectroscopy and scanning electron microscopy (SEM). The roles of location and average grain size of the alumina phase on the composite electrolyte properties were evaluated. The electrical response of the composite materials was found to be strongly influenced by the presence of a YSZ–glass interface where the motion of oxygen ions is blocked. The formation of this interface can be easily identified because of a typical relaxation frequency, much lower than those corresponding to bulk or grain boundary behavior in YSZ-based materials, or to the glass phase alone. Zirconia-based cells were also covered with a top layer of glass, and afterwards fired and electrically characterized by impedance spectroscopy. With increasing firing time at constant temperature, the relaxation frequency of the intermediate frequency arc moves from typical YSZ grain boundary behavior to lower values near to those found for the YSZ–glass interfacial response in YSZ + glass or YSZ + glass + alumina composites. This is a strong indication of the potential of impedance spectroscopy in monitoring the electrolyte corrosion process. © *1997 Elsevier Science Limited.*

1 Introduction

In recent years we have dedicated significant attention to the performance and protection of zirconia-based oxygen sensors for different types of applications.[1–4] In all cases the electrolyte was protected from the action of chemically aggressive environments. This is hardly the situation observed in many industrial applications like glass-melting furnaces. The performance of oxygen sensors in such conditions has been the subject of attention for more than 20 years.[5–9] Technical reasons (control of the oxidation state of coloring species) and economical reasons (efficient control of fuel combustion) still justify this attention. From such studies it is known that zirconia-based electrolytes are easily corroded when in direct contact with glass melts. In the case of calcia-stabilized zirconia (CSZ), the electrolyte loses calcium to the melt, causing the cubic to monoclinic transformation of zirconia. Both mechanical and electrolytic properties are lost during this process (a few hours at 1200°C).[6–8] Corrosion resistance of yttria-stabilized zirconia (YSZ) is higher than for CSZ and this justifies the preference given to the former electrolyte for the fabrication of commercial devices.

Monitoring of the electrical performance of glass–ceramic composites by impedance spectroscopy has been found to be an effective way to study interfacial phenomena and to follow developing microstructures, including the formation of new phases.[10,11] In previous work we have also used impedance spectroscopy to show that the incorporation of glass by YSZ would cause a significant change in the electrical behavior of zirconia. Such a change in behavior was due to the formation of a large YSZ–glass interfacial contact area per unit volume, blocking the motion of oxygen ions.[12,13]

Corrosion of zirconia-based electrolytes in contact with different types of melts is known to occur mostly via the grain boundaries.[14,15] Increasing the YSZ grain size was seen to be an effective way to decrease the corrosion rate.[14] These observations suggested the use of a dispersed ceramic phase at the YSZ grain boundaries, to test the effectiveness of this phase in combining chemically with the corroding medium and slowing down the corrosion process. Combination of alumina with glassy

*To whom correspondence should be addressed.

phases present in the grain boundaries of zirconia-based electrolytes is a well-known process.[16] Different products can be formed from the glass–alumina reaction, depending on the compositions involved and the experimental conditions.[16–18] Lastly, alumina particles dispersed in a zirconia matrix are also known to improve the mechanical properties of zirconia based electrolytes.[19,20] These were enough reasons for the choice of this combination of materials. Thus, the central subject of this work is a combined microstructural and electrical characterization of zirconia + glass + alumina composites. The ultimate objective is the evaluation of the role of the dispersed alumina phase (grain size and location) on the glass–YSZ interaction, and of the potential of impedance spectroscopy for the non-destructive evaluation of electrolyte degradation in YSZ sensors in glass-melting furnaces.

2 Experimental Procedure

The starting materials used to prepare the different zirconia + glass + alumina composites were YSZ powder (8 mol% Y_2O_3, from Tosoh), a green soda-lime glass (composition reported in)[13] and three different types of alumina powders. The first alumina powder (a1) had a small average grain size (< 1 μm); the second (a2) and third (a3) types of alumina powders had increasingly larger average grain sizes, up to about 10 μm. Powder (a2) was obtained from (a3) after wet milling with zirconia balls for 1 h 30 min. The grain-size distributions of these powders are shown in Fig. 1.

The process used to prepare the different glass–ceramic composites is described elsewhere.[12,13] Mixtures of all components were milled together, pressed and fired at 1500°C for 2 h. A simplified notation will be used to describe the compositions (weight percentage) of all samples (eg: 5g10a1YSZ = 5 wt% glass + 10 wt% a1 + YSZ). The resulting sintered disks were electroded with porous Pt and studied by impedance spectroscopy in air (20 Hz–1 MHz), in the range 300–800°C. As they had a homogeneous distribution of all phases along the disk axis (on a macroscopic scale), these disks will be named 'symmetrical cells'.

A specific series of experiments was performed with sintered YSZ or YSZ + alumina composite disks. These disks were covered with a layer of glass on one side and fired at 1300°C for periods of 2 or 60 h. These experiments were conceived to try to reproduce in closer detail the corrosion process of zirconia electrolytes when in direct contact with glass melts. After mechanical removal of the layer of glass and a thin top layer of the ceramic (about 100 μm thick), these disks were also electroded for electrical measurements (scheme in Fig. 2). As only one of the sides of the disk had been exposed to glass, these cells will be named 'asymmetrical cells'.

Microstructural characterization was performed on cross-sections of the different materials, after polishing and thermal etching. The evaluation of the YSZ average grain size and YSZ–glass interfacial area per unit volume followed the usual stereological characterization procedures.[21]

3 Results and Discussion

3.1 Microstructural characterization

Microstructures of zirconia + alumina composites have been studied for a long time because of their relevance to the electrical and mechanical performance of these composites. Depending on processing route and particle size, the alumina grains can be found inside zirconia grains or along grain boundaries.[19,20] A very slight solubility of alumina in the zirconia lattice is commonly assumed, but

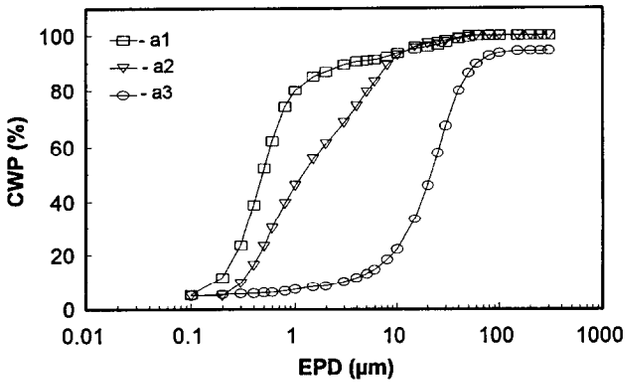

Fig. 1. Grain size distribution of the different alumina powders (a1), (a2) and (a3), expressed as the cumulative weight percentage (CWP) versus the equivalent particle diameter (EPD).

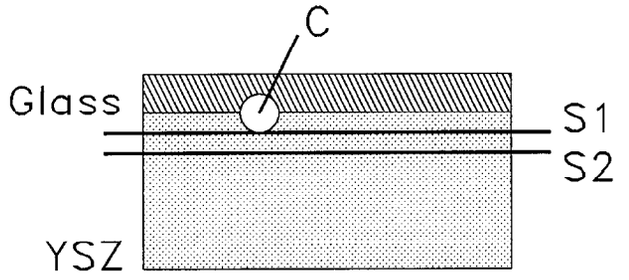

Fig. 2. Schematic view of cell layout during corrosion experiments performed with electrolyte disks fired in direct contact with glass (top layer). Lines S1 and S2 indicate the relative positions of one of the electroded surfaces of cells studied by impedance spectroscopy, after mechanical removal of the top layers of material. The second electrode was always deposited on the bottom electrolyte surface (see data shown in Figs 7–9). Microstructures shown in Fig. 4 correspond to region C.

with little impact in terms of the bulk material electrical behavior.[22] As the low electrical conductivity of alumina is well known, this means that unlike silica, alumina is not present as a continuous phase in between YSZ grains. Percolation of the alumina phase is only reached for significantly high volume fractions.[23]

Microstructures of zirconia + glass + alumina composites (5g10a1YSZ, 5g10a2YSZ and 5g10a3YSZ) were found to be coherent with previous comments (see Fig. 3). The larger alumina grains (a2) and (a3) were found dispersed throughout the matrix, covered by glass. For the composites including the smaller alumina grain size (a1), a significant fraction of alumina particles was found inside the zirconia grains and the remaining fraction at the periphery of YSZ grains. In all cases glass covered the YSZ grains in a rather uniform manner.

Simple observation of all microstructures suggests that the smaller the alumina grain size the smaller the YSZ average grain size and the larger the YSZ–glass interfacial area per unit volume. Quantitative characterization of these parameters is conclusive: the average YSZ grain size is 7·4 μm when alumina (a3) is used, and this value drops to 3·0 μm when alumina (a1) is used. The corresponding estimates for the YSZ–glass interfacial area per unit volume are $1{\cdot}1\times10^3$ and $1{\cdot}4\times10^3$ mm^2 mm^{-3}, respectively. The corresponding values for (a2) additions are close to those found for (a3) (7·3 μm and again $1{\cdot}1\times10^3$ mm^2 mm^{-3}, respectively).

The cation concentration profiles determined by EDS showed that aluminum was not displaced in detectable quantities to the other phases and that no aluminum silicates had been formed, although their formation might be expected considering previous work on similar systems.[17,18] On the contrary, yttrium was easily displaced from YSZ to the glass phase. Yttrium concentration profiles were found quite relevant to understanding the electrolyte corrosion process and developed microstructures, and will be further discussed in the following paragraphs.

With the aim of better understanding the corrosion mechanism, the zirconia-based disks (without or with alumina additions) fired in direct contact with a glass layer were also studied. As the YSZ + alumina composites based on extreme alumina grain sizes (a1) and (a3) were representative of the different types of composite microstructures, only these two composites were used in asymmetrical cell experiments. The microstructures (cross-section) of such cells are shown in Fig. 4. For long firing periods the electrolyte starts to become destroyed at the electrolyte–glass interface. EDS analysis of small loose zirconia grains near to the glass phase showed no trace of yttrium (between points (A) and (B), Fig. 4(b)), while further from the glass layer (points (C) and (D)) the composition was similar to the starting material (YSZ). This type of behavior was confirmed in every case and showed that the electrolyte degradation mechanism involves removal of yttrium from YSZ

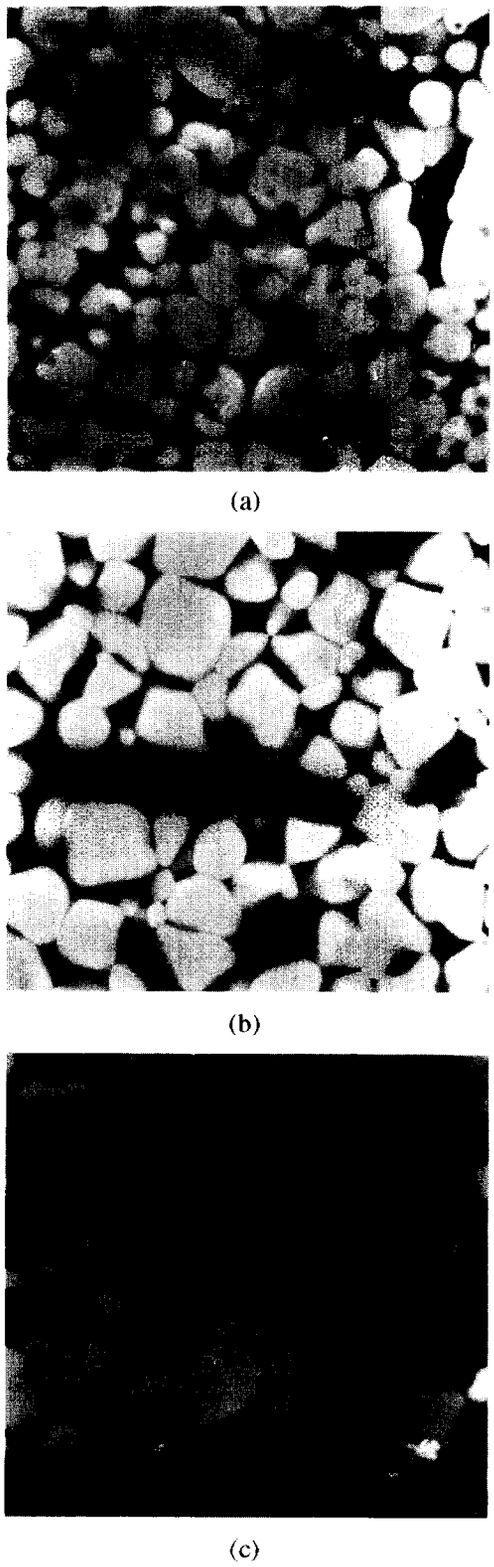

(a)

(b)

(c)

Fig. 3. Microstructures of YSZ + glass + alumina composites: (a) 5g10a1YSZ; (b) 5g10a2YSZ; (c) 5g10a3YSZ.

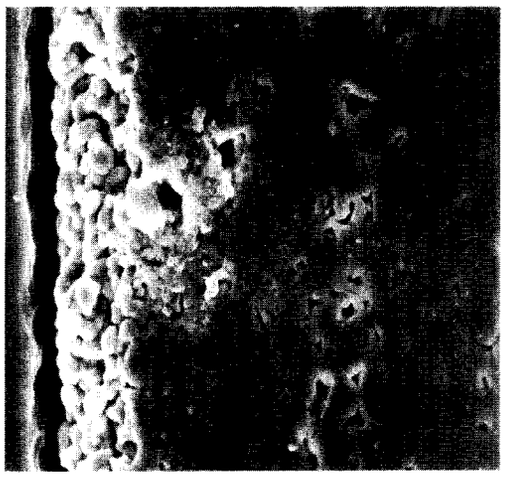

(a)

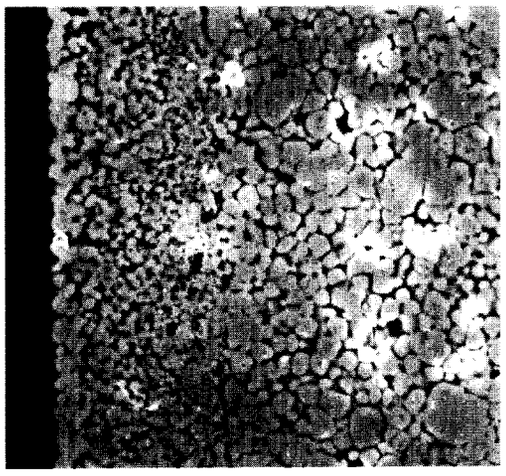

(b)

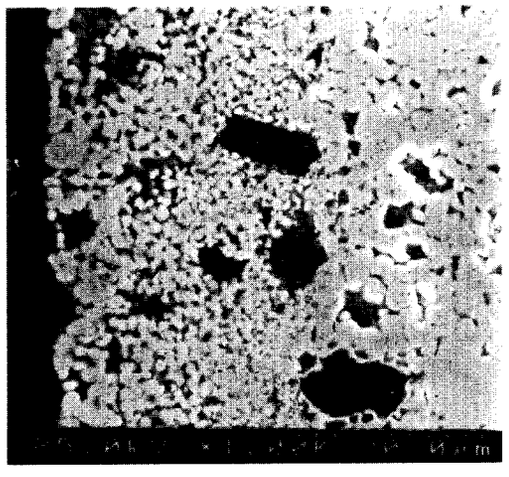

(c)

Fig. 4. Microstructures (cross-section) of (a) YSZ–glass; (b) 10a1YSZ–glass; (c) 10a3YSZ–glass cells after 60 h at 1300°C, after polishing and thermal etching (Fig. 2 for details). In (b), points (A) and (B) correspond to monoclinic zirconia (with negligible amounts of yttrium) while in (C) and (D) the cubic zirconia composition was preserved. The same transformation of the glass-exposed electrolyte layer was also observed in (a) and (c).

with transformation to monoclinic zirconia. This transformation is known to cause the fracture of the electrolyte, besides loss of electrolytic properties.

The progress of the glass via grain boundaries is much faster than removal of yttrium from the electrolyte with subsequent phase changes. This could be concluded from the observation of liquid phase at triple contact points between grains, far away (1 mm) from the glass–electrolyte interface where the presence of the monoclinic phase is already clear. This means that a YSZ sensor tube might become 'soaked' with glass before fracture. Therefore, removal of yttrium from solid solution and transformation of exposed YSZ grains to monoclinic zirconia is one aspect of the corrosion process (outer surface corrosion). Progression of glass via grain boundaries is another aspect (inner corrosion). Because of a much slower yttrium removal, both processes can be regarded as occurring in parallel. Most of the previous work on the corrosion of YSZ was focused on the quantitative determination of monoclinic zirconia formed by loss of the stabilizing agent. This corrosion process was found to be favored by small YSZ grain sizes.[14] In our context this is equivalent to the outer corrosion process, but gives no further information on the rate of progression of the corrosive agent through the electrolyte material (inner corrosion).

For YSZ disks (alumina-free) fired at 1300°C either for 2 or 60 h in contact with the glass layer, glass can be seen across the sample, while the outer, attacked layer (small grains of monoclinic phase) is about 20 μm thick. For the alumina-containing compositions, the attacked layer (outer corrosion) is not much different, although slightly exceeding the thickness reported for the alumina-free electrolyte.

The large alumina grains dispersed throughout the electrolyte phase could not be found after the attack with glass (Fig. 4(c)). However, the removal of large alumina particles is believed to have occurred during the preparation of the sample for microstructural observation (polishing and thermal etching) rather than because of reaction with glass. In fact, untreated fracture surfaces of these cells showed the presence of the alumina particles dispersed throughout the electrolyte phase, as expected. For the fine alumina particles inside YSZ grains there was no removal at all, even during polishing and thermal etching. Although it was believed that the presence of alumina particles dispersed along grain boundaries should slow down the inner corrosion process, simple microstructural observations could not provide conclusive evidence for the role of this dispersed phase in such a process.

Inner electrolyte corrosion involves glass penetration through the sintered electrolyte and transport of dissolved material in the opposite direction to the glass melt. As glass penetrates via grain boundaries, the smaller the electrolyte grain size

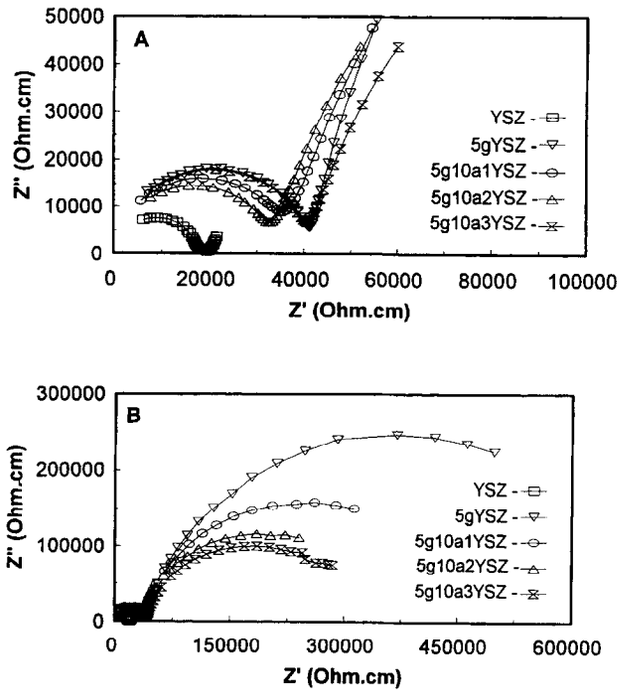

Fig. 5. Impedance spectra at 350°C of YSZ, 5gYSZ, 5g10a1YSZ, 5g10a2YSZ and 5g10a3YSZ at 350°C in air: (A) high frequency; (B) full frequency range (20 Hz-1 MHz)

the higher the number of sites and pathways for the progression of the corrosion process. Also, the smaller the YSZ grain size, the larger the total amount of glass required to 'wet' all YSZ grain boundaries. To achieve identical 'grain boundary wetting conditions' in the smaller grain-sized materials a higher flow of glass and higher accumulated amounts of glass dispersed through the electrolyte material are required. Because of the larger number of pathways for mass transport in small grain size materials (high grain boundary density) this cannot be ruled out. However, mass transport along a tortuous network of small channels is likely to be more difficult than along larger and less tortuous channels, as expected to be found in the case of larger grain-size materials. It can thus be concluded that for a given set of conditions, corrosion of external YSZ grains should be favored by the presence of small YSZ grains (quickly enveloped by glass) while glass ingress in depth might be favored by large YSZ grain sizes (large pathways with minimum tortuosity). The first conclusion is coherent with the reported role of the electrolyte grain size on the rate of cubic to monoclinic transformation, when YSZ is immersed in a corrosive agent.[14]

The idea of improved performance of YSZ + alumina composites is based on the expected blocking role of alumina particles with respect to the progression of glass. The minimum effect of alumina particles along grain boundaries would be a splitting of glass streams and increased tortuosity. This suggests that the processing route of YSZ + alumina composites should favor the location of alumina particles along grain boundaries instead of inside YSZ grains. In fact, alumina particles will also block contacts between YSZ grains, for which reason their actual role will be the result of a balance between inhibition of glass progression via grain boundaries and direct blocking of oxygen ions. Under favorable conditions (small alumina additions, with almost negligible blocking effect)[25,26] the network of continuous electrolyte–electrolyte pathways is expected to be larger for YSZ + alumina based cells because of predominant inhibition of glass progression through the electrolyte with respect to the oxygen ion blocking role of alumina particles.

3.2 Electrical characterization of symmetrical cells

The microstructural differences observed for the YSZ + glass + alumina composites should lead to different electrical behavior. In fact, for polycrystalline electrolytes characterized within a limited frequency range, impedance spectra usually consist of three major arcs, observation of which strongly depends on temperature. The high-frequency arc is usually ascribed to the bulk material behavior, the intermediate frequency arc is related to the grain boundary behavior while the lower frequency arc is due to electrode polarization processes. The presence of glassy phases causes a significant enhancement of the grain-boundary arc.[23,25] As mentioned, for simple alumina additions this dispersed phase causes a localized blocking effect. In this case the impedance spectra show significant enhancement of the high frequency and intermediate frequency arcs, the latter being the most affected by these additions. Analysis of the impedance spectra showed a close relationship between composition (volume fraction), dispersed particle size and electrical behavior.[24,26] Considering the composite nature of the materials being studied in this work, and the complex effect of each individual phase on the different impedance arcs, in the following discussion the designations 'bulk' and 'grain boundary' arcs will be replaced by 'high' and 'intermediate' frequency arcs. Comments will be made on the deviations of these arcs from perfect RC behavior, using the depression angle (β) as a measure of this deviation.[24]

Figure 5 describes the effects of glass and combined glass + alumina additions to YSZ, in terms of impedance spectra. Figure 5(A) (high frequency) and Fig. 5(B) (full range) show that the addition of glass to YSZ caused an increase in the size of both arcs (high and intermediate frequency) the intermediate frequency arc being the most affected. Figure 5(B) also shows that all alumina additions

caused an enormous decrease in the size of the intermediate frequency arc when compared to the 5gYSZ composition. In this case the role of alumina particles at intermediate frequencies resembles the usually named 'scavenger effect'[16]. However, due to the large amount of glass available, this explanation is unsatisfactory.

Figures 5(A) and (B) also describe the effect of the different alumina grain sizes on the behavior of the composite materials. While all additions were effective in decreasing the magnitude of the intermediate frequency arc, the composites based on the larger alumina grains (a2) and (a3) showed a better performance. This can be related to the reported microstructures. For additions (a2) and (a3), the location and role of the dispersed phase are similar: the average YSZ grain size is large and the YSZ–glass interfacial area is small. For the addition (a1), the electrolyte grain size is small and the YSZ–glass interfacial area is high. The latter parameter is believed to be essential in determining the magnitude of the observed intermediate frequency arc. In fact, this arc shows only a relatively small depression, with β values in the order of 10–15°. This means that although a deconvolution into two or more contributions might be attempted, there is clearly one process which dominates this contribution and the most obvious correlation is with the YSZ–glass interfacial area per unit volume.

Relaxation frequencies can be used as an indication of transition between dominant interfacial phenomena. Figure 6 shows the Arrhenius plots of the relaxation frequencies observed for all arcs and all symmetrical cell compositions. The 1gYSZ cell behavior (relaxation frequency of the intermediate frequency arc) is clearly between the 'pure' YSZ grain boundary behavior and the behavior of cells with higher glass content (2gYSZ and 5gYSZ).

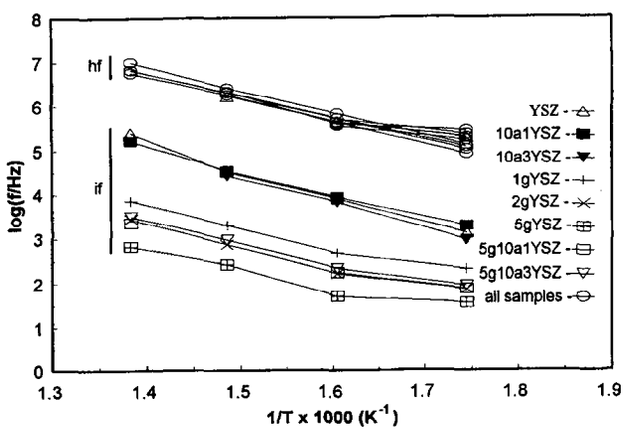

Fig. 6. Arrhenius plots of relaxation frequencies of impedance arcs observed for symmetrical cells. High frequency (hf) arc (all cells): ○. Intermediate frequency (if) arc: glass free cells—Δ and filled symbols; glass containing cells +, × and remaining open symbols.

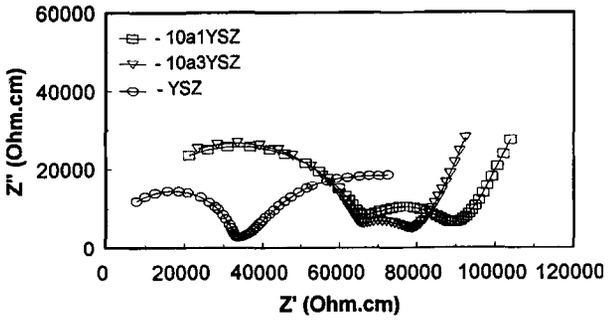

Fig. 7. Impedance spectra at 350°C (corrected for the different cell thicknesses) of YSZ, 10a1YSZ and 10a3YSZ disks after firing for 2 h at 1300°C, with a top layer of glass (section S1 in Fig. 2).

Furthermore, the relaxation frequencies of the intermediate frequency arcs observed for YSZ or YSZ + alumina composites are near to those found for the YSZ grain boundary behavior, and are at least one order of magnitude higher than those observed for the glass-containing composites. This shift in relaxation frequency with composition (glass content) clearly indicates a transition between dominant interfacial phenomena.

3.3 Electrical characterization of asymmetrical cells

The experimental conditions used in processing the symmetrical cells previously described are far from those typical of sensor applications in glass-melting furnaces. In the case of immersed sensors, glass penetrates through the electrolyte. while the external YSZ grains might be lost to the glass melt, before or after loosing the stabilizing agent (yttria). Even for sensors exclusively in contact with the gas phase (either in the furnace chamber or in the heat recovery system), the high concentration of oxide vapors and particles in the atmosphere will have a similar effect. Deposited particles or condensed oxides will attack the electrolyte, the major differences from immersed sensors being compositional (oxide vapors and/or particles versus melted glass) and kinetic (mass transport mechanisms to and from the electrolyte), besides temperature. This has been confirmed after inspection and electrical characterization of YSZ disks placed in contact with a glass-melting furnace atmosphere for a period of a few weeks.

Tests were performed with asymmetrical cells (scheme in Fig. 2) in order to approach the typical sensor working conditions more closely. Figures 7 and 8 show the impedance spectra (corrected for the cell thickness) of YSZ, 10a1YSZ and 10a3-YSZ-based asymmetrical cells after being fired for 2 or 60 h at 1300°C in direct contact with a layer of glass covering one of the sides of the electrolyte disk. The spectra were obtained after removal of the top layer of glass and some electrolyte with SiC

sand paper (section S1 in Fig. 2). Although not shown, a second series of spectra was obtained after additional removal of another layer of electrolyte (section S2 in Fig. 2). The thickness of these layers (about 100 μm each) was measured by difference from the initial cell thickness (before attack with glass). From previously reported microstructures, it is believed that cells processed in this manner were free of any loose monoclinic zirconia grains. In fact, the observed microstructures suggest that such layers did not exceed 20–30 μm (see Fig. 4). Also, the trends observed in electrical behavior in consecutive measurements with thinner cells (sections S1 and S2) were found to be reproducible and roughly independent of the cell thickness.

A first point to notice is that the high frequency and intermediate frequency arcs are now within the same order of magnitude, contrary to the spectra shown in Fig. 5. Besides this fact, comparison of these impedance spectra with those reported for the symmetrical cells seems to indicate that some of the features observed with the composites YSZ + alumina + glass are repeated here. The high frequency arc is always smaller for the YSZ-based asymmetrical cells (as it was for the equivalent symmetrical cells). Also, the intermediate frequency arcs for the asymmetrical cells based on YSZ + alumina composites are smaller than observed for the alumina-free composition. Furthermore, the magnitude of the intermediate frequency arc is smaller for the (a3)-containing cell. All these features have already been reported for the symmetrical cells. The most obvious explanation is that glass penetrated through the cells and the overall result is a composite with electrical performance approaching that obtained simply by mixing and firing glass-containing mixtures (symmetrical cells).

The same general trends are observed for long and short thermal treatments. However, the larger the duration of the attack the larger the increase in magnitude of the intermediate frequency arc. Comparison of microstructures obtained for YSZ + glass + alumina composites with the asymmetrical cells show large differences. In the first case it can be said that every single electrolyte grain is surrounded by glass. In the latter case, pockets of glass between electrolyte grains coexist with more or less clean contacts between YSZ grains. This suggests that the result of the inner corrosion process is a composite with two parallel electrical pathways for electrical transport between grains. The first one (direct contact between YSZ grains) should resemble the usual interfacial behavior of the electrolyte grain boundary. The second pathway is dominated by the YSZ–glass interfacial behavior. The combination of these two parallel pathways can be regarded as an association of two parallel RC circuits, with different characteristic frequencies. As the corrosion process progresses, the number of direct contacts between YSZ grains decreases and the system moves to the characteristic performance of the YSZ + glass + alumina composites. This explains the increase in magnitude of the intermediate frequency arcs with increasing firing time. The coexistence of such parallel circuits (with different characteristic relaxation frequencies) and pathways explains why the depression angle reaches values of 20–30° (sometimes even higher) in the case of asymmetrical cells, much larger than those observed for the symmetrical cells (10–15°).

3.4 Monitoring of corrosion by impedance spectroscopy

Direct comparison between microstructures of asymmetrical cells (Fig. 4) was found inconclusive in terms of corrosion. The thickness of the outer attacked layer (monoclinic zirconia) was similar in all cases (20–30 μm). Only the average YSZ grain sizes in these samples were clearly different, being maximum for the alumina-free cell. Thermal etching used to emphasize microstructural features might be misleading in terms of identification of glass penetration depth through the electrolyte (inner corrosion).

The spectra shown in Fig. 5 suggested a number of differences related to the cell composition and provided a first basis for a positive identification of the formation of YSZ–glass interfaces, during the inner corrosion. In Fig. 5, with increasing coverage of YSZ grains by glass, the intermediate frequency arc increased in magnitude and the relaxation frequency shifted to lower values. Asymmetrical cells studied by impedance spectroscopy (Figs 7 and 8) were not far different from the symmetrical cells, as the top layer of the electrolyte had been mechanically removed. Their impedance spectra should be representative of the condition of the electrolyte in

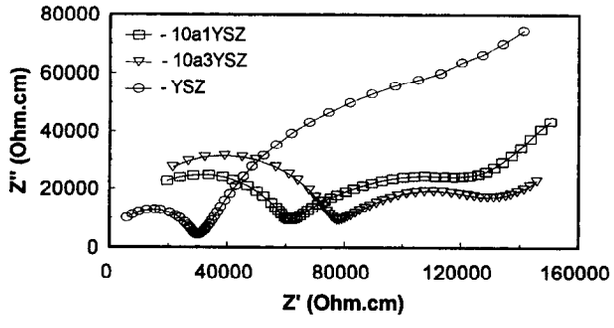

Fig. 8. Impedance spectra at 350°C (corrected for the different cell thicknesses) of YSZ, 10a1YSZ and 10a3YSZ disks after firing for 60 h at 1300°C, with a top layer of glass (section S1 in Fig. 2.

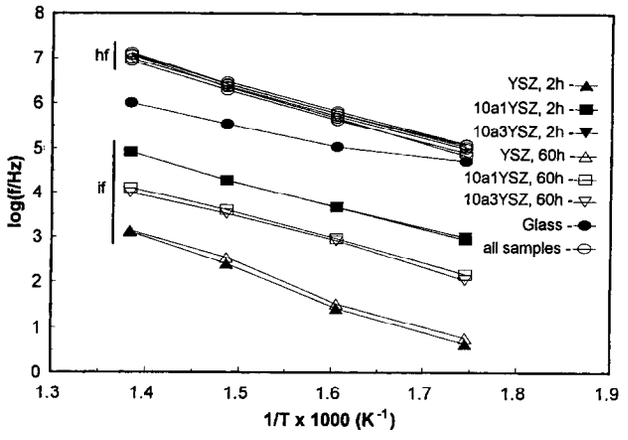

Fig. 9. Arrhenius plots of relaxation frequencies of impedance arcs observed for asymmetrical cells. High frequency (hf) arc: ○ (all cells). Intermediate frequency (if) arc: remaining symbols. Also shown data obtained for a simple disk of glass (●).

terms of inner corrosion. Therefore, the potential of impedance spectroscopy for monitoring the inner corrosion process should also be tested by analysis of the relaxation frequencies of the different impedance arcs shown in Figs 7 and 8. For this purpose, the conclusions drawn from analysis of Figs 5 and 6 will be used. This is complementary to the previous discussion on the effect of cell composition and duration of attack on the relative importance of the different impedance arcs.

Figure 9 shows the Arrhenius plots of the relaxation frequencies of the high and intermediate frequency arcs for all asymmetrical cells: YSZ–glass, 10a1YSZ–glass and 10a3YSZ–glass cells. Data corresponding to a single layer of glass is also shown for comparison. Figure 9 should be compared with Fig. 6. As observed in the latter figure, all impedance spectra include a high-frequency contribution typical of the YSZ bulk grain behavior. This arc might be more or less influenced by the presence of the remaining phases, but the relaxation frequency is about the same for every

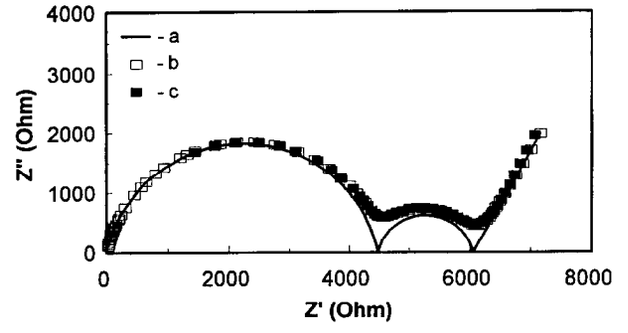

Fig. 10. Relationship between experimental data (c) and assumed model behavior. Solid lines (a) correspond to the individual impedance contributions obtained from data analysis, while the open symbols (b) describe the sum of these contributions. Experimental points correspond to data reported in Fig. 6 for the cell based on 10a1YSZ, before correction for the cell thickness.

composition and type of cell. This had already been noticed in the literature in the case of YSZ + alumina composites.[24]

At intermediate frequency, however, for the YSZ + alumina based cells, a shift in relaxation frequency is now observed: in all cases the relaxation frequency is smaller for longer periods of attack (60 h versus 2 h). The relaxation frequencies for the YSZ-based materials were the lowest and were almost the same for the two attack periods (60 h and 2 h). Following the idea that the intermediate frequency arc tends to be dominated by the electrical response of the YSZ–glass interface, this suggests that the inner corrosion of the YSZ-based cell was much faster than for cells based on the YSZ + alumina composites. This is coherent with the previous remark on easier transportation of glass through grain boundaries of larger grain-sized materials without dispersed alumina. The shift in relaxation frequencies could thus be used as an indirect test for the degree of inner electrolyte corrosion.

A great deal of the previous discussion was based on the analysis of the relaxation frequencies of the high and intermediate frequency arcs of the impedance spectra. It seems reasonable to comment on the relative accuracy of the data analysis procedure. Filled symbols in Fig. 10 correspond to data obtained with the asymmetrical cell based on 10a1YSZ, shown in Fig. 6. In this case (Fig. 10), the spectrum includes the raw data (cell impedance), while Fig. 6 included the same data but corrected for the cell thickness. This explains the different units and orders of magnitude. Also shown in Fig. 10 are the individual contributions considered in fitting the experimental data (solid lines), and the sum of these individual contributions (open symbols). The agreement is very good in this and in the other cases. This means that the shift in orders of magnitude of relaxation frequency with composition or experimental conditions cannot be ascribed to a large uncertainty in the fitting procedure. This could already be assumed because of the well-defined spectra shown in all figs.

No comment has yet been made on the specific process controlling this relaxation frequency. While experimental evidence suggests that it is related to the YSZ–glass interfacial behavior, it should also be noticed that the observed relaxation frequencies are well below those typical of YSZ grain boundaries and are comparable to relaxation frequencies typical of electrode processes. It is believed that these impedance contributions are caused by the interfacial reaction occurring at the YSZ–glass interface, which is more than a simple transport process across one interface. Oxygen ions

are known to be able to become incorporated in the glass phase, but their mobility in this phase is quite small. Instead, in the glass phase the most mobile ionic species are likely to be cations. The process of ionic transport across the whole composite involves a change in charge-carrying species, and this change occurs at the electrolyte–glass interface which is easily polarizable. For this reason this interfacial polarization will tend to be significant if compared to the usual interfacial processes occurring in grain boundaries.

4 Conclusions

For extremely severe conditions (high temperatures or long thermal treatments), yttrium is displaced from the electrolyte (YSZ) to the glass phase, causing the formation of monoclinic zirconia and mechanical disruption of the electrolyte sintered body. However, in parallel, glass also progresses via grain boundaries and the electrical performance of the electrolyte is affected because of the formation of new types of interfaces (electrolyte–glass). Impedance spectroscopy was used to monitor this inner corrosion process taking advantage of the formation of this new interface, which had a specific electrical effect. In fact, a large shift in the relaxation frequency of the cell intermediate frequency impedance arc can be used to monitor the progress of glass through the electrolyte. Dispersed alumina particles are believed to slow down this process, but a minimum alumina grain size and controlled processing conditions are required to ensure that alumina grains lie along grain boundaries where their role is maximum.

Acknowledgement

Work was partly funded by PRODEP 2 (Portugal).

References

1. Marques, F. M. B. and Wirtz, G. P., Oxygen fugacity control in non-flowing gas phase systems. I–Experimental Results. *J. Am. Ceram. Soc.*, 1992, **75**(2), 369–374.
2. Wirtz, G. P. and Marques, F. M. B., Oxygen fugacity control in non-flowing gas phase systems. II–Theoretical Model. *J. Am. Ceram. Soc.*, 1992, **75**(2), 375–381.
3. Costa, A. D. S., Labrincha, J. A. and Marques, F. M. B., Performance of protected oxygen sensors. Part I: single phase mixed conducting filters. *Solid State Ionics*, 1995, **81**, 73–83.
4. Costa, A. D. S., Labrincha, J. A. and Marques, F. M. B., Performance of protected oxygen sensors. Part II: short circuited electrochemical filters. *Solid State Ionics*, 1995, **81**, 85–96.
5. Brown, J. T., Hoskins, J. W., and Chirino, A. M., Continuous oxygen measurement in tank combustion atmospheres.*The Glass Industry*. 1976, 12–15.
6. Tran, T. and Brungs, M. P., Applications of oxygen electrodes in glass melts. Part 1: oxygen reference electrode. *Phys. Chem. Glasses*, 1980, **21**(4), 133–140.
7. Tran, T. and Brungs, M. P., Applications of oxygen electrodes in glass melts. Part 2: oxygen probes for the measurement of oxygen potential in sodium disilicate glass. *Phys. Chem. Glasses*, 1980, **21**(5), 178–183.
8. Tran, T. and Brungs, M. P., Applications of oxygen electrodes in Glass melts. Part 3: an oxygen concentration cell for thermodynamic studies of CO-CO_2 and Ni-NiO Systems. *Phys. Chem. Glasses*, 1980, **21**(5), 184–188.
9. Ji, J. J. and Brungs, M. P., A Probe for measuring oxygen activity in molten glasses, In *Science and Technology of Zirconia V*, ed. S. P. Badwall, M. J. Bannister, R. H. J. Hannink. Technomic Publ. Co., Inc., PA, 1994, 623–628.
10. Adams, St., Hariharan, K. J. and Maier, J., Interface effect on the silver ion conductivity during crystallization of AgI-Ag_2O-V_2O_5 glasses. *Solid State Ionics*, 1995, **75**, 193–201.
11. Grincourt, Y., Coppo, D., Souquet, J.-L. and Duclot, M., Impedance spectroscopy applied to annealing effects on glassy $AgPO_3$: sub T_g surface crystallisation and glass relaxation. *Phys. Chem. Glasses*, 1995, **36**(3), 123–126.
12. Rodrigues, C. M. S. Labrincha, J. A. and Marques, F. M. B., Degradation of zirconia based sensors in glass melting furnaces, Ionics, 2, 1996, 12–18.
13. Rodrigues, C. M. S., Labrincha, J. A. and Marques, F. M. B. Electrical behavior of zirconia-alumina-glass composites. In *Electroceramics V, Book 2*, ed. J. L. Baptista, J. A. Labrincha and P. M. Vilarinho, Fund. JJM, Aveiro, 1996, 135–138.
14. Stournaras, C. J., Tsetsekou, A., Zambetakis, Th., Kontoyannis, C. G. and Carountzos, G., Corrosion of yttria-fully stabilized zirconias in molten fluorides. *J. Mat. Sci.*, 1995, **30**, 4375–4379.
15. Tagawa, H., Mizusaki, J., Hamano, H. and Shimada, M. Corrosion of stabilized zirconia with alkali metal carbonates. In *Science and Technology of Zirconia V*, ed. S. P. Badwall, M. J. Bannister, R. H. J. Hannink. Technomic Publ. Co., Inc., PA, 1994, 847–854.
16. Buttler, E. P. and Drennan, J., Microstructural analysis of sintered high-conductivity zirconia with Al_2O_3 additions. *J. Am. Ceram. Soc.*, 1982, **65**(10), 474–478.
17. Imanaka, Y., Aoki, S., Kamehara, N. and Niwa, K., Cristobalite formation in glass/ceramic composites. *J. Am. Ceram. Soc.*, 1995, **78**(5), 1265–1271.
18. Park, J.-H. and Lee, S.-J., Mechanism of preventing crystallization in low-firing glass/ceramic composite substrates. *J. Am. Ceram. Soc.*, 1995, **78**(4), 1128–1130.
19. Ishizaki, F., Yoshida, T. and Sakurada, S. Effect of alumina additions on the electrical properties of yttria-doped zirconia In *Proc. 1st. Int. Symp. on SOFCs*, ed. S. C. Singhal. The Electrochemical Soc. Inc., Pennington, 1989 3–14.
20. Yamamoto, O., Takeda, Y., Imanishi, N., Kawahara, T., Shen, G. Q., Mori, M. and Abe, T. Electrical amd mechanical properties of zirconia-alumina composite electrolyte. In *Proc. 2nd. Int. Symp. on SOFCs*, ed. F. Gross, P. Zegers, S. C. Singhal and O. Yamamoto. CEC, Brussels, 1991 437–444.
21. Underwood, E. E. Quantitative stereology, Addison-Wesley Publishing Co., Georgia, 1970.
22. Miyayama, M., Yanagida, H. and Asada, A., Effects of Al_2O_3 additions on resistivity and microstructure of yttria-stabilized zirconia. *Am. Ceram. Soc. Bull.*, 1985, **64**(4), 660–664.
23. Schouler, E. Study of oxide solid electrolyte based cells by the complex impedance technique—application to the accurate measurement of conductivity and to the study of the oxygen electrode reaction. Ph. D. thesis, Institut National Polytechnique de Grenoble (INPG), Grenoble, 1979.
24. Steil, M. C., Thevenot, F., Dessemond, L. and Kleitz, M., Impedance spectroscopy analysis of conduction percolation in zirconia-alumina compostes. In *3rd Euro-Ceramics*,

Vol. 2, ed. P. Duran and J. F. Fernandez. Faenza Editrice Iberica S.L., Castellon de la Plana, 1993 271–280.
25. Bernard, H. Microstructure and conductivity of sintered stabilized zirconia. Ph. D. Thesis, Institut National Polytechnique de Grenoble (INPG), Grenoble, 1980.
26. Kleitz, M., Djurado, E., Robert, P. O., Steil, M. C. and Thevenot, F. Impedance spectroscopy analysis of the electric behavior of ceramic composites. In *Electroceramics IV*, Vol. 2, ed. R. Waser, S. Hoffmann, D. Bonnenberg and Ch. Hoffman, Augustinus Buchlandlung, Aachen, 1994 725–732.